Journal Pre-proof

GSDMD membrane pore is critical for IL-1β release and antagonizing IL-1β by hepatocyte-specific nanobiologics is a promising therapeutics for murine alcoholic steatohepatitis

Jingyun Luan, Wei Chen, Jiajun Fan, Shaofei Wang, Xuyao Zhang, Wenjing Zai, Xin Jin, Yichen Wang, Zhenyi Feng, Jinghui Zhang, Ming-Lin Liu, Dianwen Ju

PII: S0142-9612(19)30669-6

DOI: https://doi.org/10.1016/j.biomaterials.2019.119570

Reference: JBMT 119570

To appear in: *Biomaterials*

Received Date: 2 July 2019

Revised Date: 16 October 2019

Accepted Date: 18 October 2019

Please cite this article as: Luan J, Chen W, Fan J, Wang S, Zhang X, Zai W, Jin X, Wang Y, Feng Z, Zhang J, Liu M-L, Ju D, GSDMD membrane pore is critical for IL-1β release and antagonizing IL-1β by hepatocyte-specific nanobiologics is a promising therapeutics for murine alcoholic steatohepatitis, *Biomaterials* (2019), doi: https://doi.org/10.1016/j.biomaterials.2019.119570.

GSDMD Membrane Pore is Critical for IL-1β Release and Antagonizing IL-1β by Hepatocyte-Specific Nanobiologics is a Promising Therapeutics for Murine Alcoholic Steatohepatitis

Jingyun Luan[1,2#], Wei Chen[1,2#], Jiajun Fan[1,2], Shaofei Wang[1,3], Xuyao Zhang[1,3], Wenjing Zai[1,2], Xin Jin[1,2], Yichen Wang[1,2], Zhenyi Feng[1,2], Jinghui Zhang[4], Ming-Lin Liu[5,6*], Dianwen Ju[1,2*]

[1]Department of Microbiological and Biochemical Pharmacy& The Key Laboratory of Smart Drug Delivery, Ministry of Education, School of Pharmacy, Fudan University, Shanghai, 201203, P. R. China

[2]Minhang Hospital, Fudan University, 170 Xinsong Road, Shanghai 201199, China

[3]Department of Systems Pharmacology and Translational Therapeutics, Perelman School of Medicine, University of Pennsylvania, Philadelphia, PA 19104, USA

[4]Department of Gastrointestinal Surgery, Changhai Hospital, The Second Military Medical University, Shanghai, 200433, China

[5]Department of Dermatology, Perelman School of Medicine, University of Pennsylvania, Philadelphia, PA 19104, USA

[6]Corporal Michael J. Crescenz VAMC, Philadelphia, PA 19104, USA

[#]These authors contributed equally to this work.

***Corresponding author**: Ming-Lin Liu (E-mail: lium1@pennmedicine.upenn.edu)

Dianwen Ju (E-mail: dianwenju@fudan.edu.cn)

Abstract

Excessive release of interleukin-1β (IL-1β) is well-known to provoke cascades of inflammatory responses thus contributing to the pathogenesis of alcohol-induced steatohepatitis (ASH), but the cellular mechanism that regulates IL-1β release during ASH remains unclear. Herein, we identified that gasdermin D (GSDMD) membrane pore is critical in mediating IL-1β hypersecretion from chronic ethanol or acetaldehyde-stimulated macrophages. Deletion of GSDMD reduced IL-1β release and ameliorated alcoholic steatohepatitis *in vivo*. These findings uncovered a novel mechanism regarding the IL-1β release in ASH, and also indicated the therapeutic potential of IL-1β blockade. Interleukin-1 receptor antagonist (IL-1Ra) is protective to ASH by blocking IL-1β, but it has a short biological half-life (4-6 h) and lower liver concentrations. Thus, we constructed a therapeutic plasmid pVAX1-IL-1Ra-ApoAI (pVAX1-IA) encoding IL-1Ra anchored to the liver-targeting protein apolipoprotein A-I (ApoAI), and developed hepatocyte-specific nanobiologics (Glipo-pVAX1-IA) by galactose functionalization for local and prolonged expression of IL-1Ra in liver. Data presented here showed that Glipo-pVAX1-IA facilitated efficient uptake of gene cargos by hepatocytes. The biodistribution studies confirmed a predominant hepatocytes internalization, but a minimal kupffer cells uptake of Glipo-pVAX1-IA following intravenous injection. The locally secreted IL-1Ra attenuated alcohol-induced steatohepatisis and infiltration of inflammatory cells. Together, our results unraveled the critical role of GSDMD membrane pore in IL-1β hypersecretion and highlighted the hepatocyte-specific Glipo-pVAX1-IA nanobiologics as a

promising therapeutic strategy for ASH.

Keywords: interleukin-1β, gasdermin D, interleukin-1 receptor antagonist, apolipoprotein A-I, galactose, alcohol-induced steatohepatitis

1. Introduction

Alcohol consumption causes approximately 3.3 million deaths (5.9% of total) worldwide each year, in which alcoholic liver disease (ALD) occupies the most majority [1]. Alcohol-induced steatohepatitis (ASH) is a life-threatening inflammatory disorder that occurs in ALD patients with a recent excessive alcohol consumption, characterized by massive lipid accumulation and dysregulated inflammatory responses in liver [2,3]. Therapeutic options including glucocorticoids, phosphodiesterase inhibitors and anti-tumor necrosis factor-α (TNF-α) agents are now available, but very little success has been achieved in the therapy of ASH [4,5]. Thus, works aim at explore novel therapeutic strategies are urgently required. Recently, the proinflammatory cytokine interleukin-1β (IL-1β) has received special attentions for its role in initiating the cascade of events leading to ASH [6-11]. It participates in lipid synthesis in hepatocytes, and promotes the infiltration of inflammatory cells and secretion of other cytokines in liver. In particular, genetic deletion of regulators of IL-1β maturation protected mice from alcohol-induced liver injury and steatosis [7]. These studies provided evidences for the significant role of IL-1β in the development of ASH. Therefore, understanding the cellular mechanism that regulates the IL-1β release and development of IL-1β-targeted therapeutics would be important for ASH treatment.

IL-1β is not secreted through the conventional endoplasmic reticulum (ER)-Golgi route of protein secretion, and the mechanism of its release in ASH remains unclear [12]. Few latest studies from several groups have demonstrated that

the cytosolic gasdermin D (GSDMD) can be activated and translocated to plasma membrane where the GSDMD-N polymer formed membrane pores, which are critical for release of mature IL-1β [13-15]. However, it is not well-understood if GSDMD also mediates IL-1β release in ASH, which would be addressed with *GSDMD*$^{-/-}$ mice in the current study.

The importance of IL-1β in the pathogenesis of ASH implied the therapeutic potential of IL-1β blockade. Interleukin-1 receptor antagonist (IL-1Ra) functions as a competitor of IL-1β to block interleukin-1 receptor type 1 (IL-1R1)-mediated intracellular signaling pathway [16]. The remarkable anti-inflammatory efficacy of IL-1Ra has already been well documented, and its clinical trial on severe acute alcoholic hepatitis is currently ongoing (NCT01809132) [17]. However, some limitations are required for attention to optimize the practical applications of IL-1Ra. The most important limitation of IL-1Ra is its short half-life (4-6 h) due to the rapid clearance from kidney [18,19]. To cope with this problem, several attempts have been made to extend the persistence of IL-1Ra in the circulation, either by development of pegylated IL-1Ra or fusion it with other large proteins such as elastin-like polypeptides [20,21]. Nonetheless, these modifications are compromised by the lack of hepatic tropism, a character that is preferential for treating liver diseases. Moreover, systemic administration of IL-1Ra is accompanied by the risk of decreased host defenses due to the widespread spread of IL-1R1 [22,23]. Therefore, strategies that combine both sustained release of IL-1Ra and increased liver tropism are urgently needed.

Apolipoprotein A-I (ApoAI), an important component of high-density lipoproteins, has been proposed as a promising candidate for selective liver targeting [24]. Upon binding of scavenger receptor class B type I (SR-BI) that efficiently expresses on the cell membrane of hepatocytes, ApoAI facilitates the delivery of cholesterol from peripheral organs to hepatocytes [25]. It has been demonstrated that ApoAI predominately distributed in the liver after systemic administration [26]. Moreover, linkage of ApoAI to other proteins, such as interferon-α, interleukin-15 and interleukin-22, showed promising liver targeting, prolonged duration and reduced immunological side effects [27-29]. Inspired by these attractive features, we hypothesized that IL-1Ra anchored to ApoAI may both prolong the lifetime of IL-1Ra and realize liver targeting, but is devoid of side effects induced by widespread IL-1R1 blockade.

In order to increase the active uptake of hepatocytes, we took advantage of galactose, which has strong affinity to asialoglycoprotein receptor (ASGPR) on hepatocytes [30-32]. We firstly tethered IL-1Ra to ApoAI to construct a eukaryotic expression plasmid pVAX1-IL-1Ra-ApoAI (pVAX1-IA) and developed hepatocyte-specific nanobiologics (Glipo-pVAX1-IA) for local and prolonged expression of IL-1Ra to prevent ASH. In the nanobiologics, cationic liposomes composing of 1, 2-dioleoyl-3-trimethylammonium-propane (DOTAP) and cholesterol provided positive-charge for encapsulation of negatively charged pVAX1-IA, and galactose modification on lipid bilayer was to facilitate hepatocyte-specific delivery of therapeutic IL-1Ra. Furthermore, the stability, kinetic behaviors and the potential

therapeutic efficacy of the nanobiologics were also evaluated. Results from our study highlighted that Glipo-pVAX1-IA would be a promising therapeutic approach to treat ASH. Taken together, the current study elucidated the cellular mechanism that regulates IL-1β release and also developed IL-1β-targeted therapeutics for ASH.

2. Methods

2.1. Materials

DOTAP and 1, 2-distearoyl-sn-glycero-3-phosphoethanolamine (DSPE) were obtained from Avanti Polar Lipids (Alabaster, Canada). Galactose-polyethyeneglycol$_{34000}$-NHS (Galactose-PEG-NHS) and polyethyeneglycol$_{34000}$-NHS (PEG-NHS) were obtained from JenKem Technology (Beijing, China). Cholesterol was obtained from Sigma-Aldrich (St. Louis, USA). Plasmid pCMV- enhanced green fluorescent protein (EGFP) was from Beyotime Institute of Biotechnology (Haimen, China). FAM-FLICA Caspase-1 Assay Kit was purchased from ImmunoChemistry (Minnesota, USA). Leukocyte Activation Cocktail (with Gologi Plug) and percoll were obtained from BD Bioscience (Franklin Lakes, USA). The eukaryotic expression plasmid pVAX1, lipofectamine 2000, Hoechst 33342, lyso-tracker green, and TOTO-3 were obtained from Thermo Fisher (Waltham, USA). For western blot and immunohistochemical analysis, antibodies against GSDMD (ab209845), IL-1Ra (ab124962), ApoAI (ab52945) and Gr-1 (ab25377) were from Abcam (Cambridge, UK), and IL-1β (12242), β-actin (4970) and GAPDH (51332) were from Cell Signaling Technology (Danvers, USA).

2.2. Mice and animal model

Mice were grown under specific pathogen free conditions, and all procedures involving animals were carried out according to standards approved by the Animal Ethical Committee of School of Pharmacy at Fudan University. *GSDMD*$^{-/-}$ mice on the C57BL/6 background had been described before [13]. Nine to ten weeks old, female wide type (WT) or *GSDMD*$^{-/-}$ mice on the C57BL/6 background were exposed to Lieber-DeCarli liquid diet (TP4030D, Trophic, China) with 5% ethanol for 10 days plus a single binge ethanol (5 g/kg body weight). For control mice, an isocaloric alcohol-free diet (TP4030C, Trophic, China) was given in the identical manner, and a single binge of isocaloric dextrin maltose were then administrated by gavage. Various nanobiologics were intravenously injected at a dose of 50 μg of pVAX1-IA every three day. Mice were sacrificed at 9 h post ethanol gavage, and serum and liver tissues were carefully harvested. The levels of IL-1β and interleukin-17A (IL-17A) in serum and liver were assessed using ELISA kit following the manufacturer's instruction.

2.3. Immunofluorescence analysis

Paraffin-embedded liver sections were deparaffinized and antigen-retrieved for immunofluorescence analysis. Specimens were incubated with hamster anti-IL-1β (Sc-12742, Santa Cruz Biotechnology) and rabbit anti-GSDMD (abx340202, Abbexa) antibody at 4°C overnight, and then stained with AF647-goat anti-Armenian Hamster IgG (ab173004, Abcam) and AF488-goat anti-rabbit IgG (ab150077, Abcam) antibody for 1 h at room temperature. After blocking with 3% bovine serum albumin, specimens were probed with rabbit anti-F4/80 (ab100790, Abcam) antibody at 4°C overnight and AF546-goat anti-rabbit IgG secondary antibody (A11010, Thermo

Fisher) for 1 h at room temperature. Liver tissues were counterstained with Hoechst 33342 and imaged by confocal microscope LSM710 (ZEISS, Jena, Germany).

2.4. Th17 cells assay

Nonparenchymal liver cells were isolated using discontinuous 40%/70% percoll density gradient centrifugation, and then stimulated with leukocyte activation cocktail (with BD Gologi Plug) at 37°C for 5 h. After staining with APC-labeled CD4 antibody (100516, Biolegend) for 12 h at 4°C, cells were fixed, permeabilized and stained with PE-labeled IL-17A antibody (506903, Biolegend) at 4°C for 2 h. The amount of Th17 cells were measured using flow cytometry (FACSCalibur, BD Biosciences, USA).

2.5. Cell culture and treatments

HepG2, Huh7 and HEK-293T cells were purchased from Chinese Academy of Sciences and cultured following standard protocals. Bone-marrow-derived macrophages (BMDMs) were isolated from 8-10 weeks old WT or *GSDMD*$^{-/-}$ mice, and then differentiated in the presence of 20 ng/ml recombinant macrophage colony-stimulating factor for 7 days. BMDMs were seeded in 96-well plates (1×10^5 cells/well) and 6-well plates (2×10^6 cells/well). The fully differentiated BMDMs were exposed to ethanol (100 mM and 200 mM) or acetaldehyde (0.1 mM and 1 mM) for 72 h. After stimulating with LPS (100 ng/ml) in ethanol- or acetaldehyde-free medium for 5 h, BMDMs were then treated with 5 mM ATP (S1985, Selleckchem, USA) for 1 h. The secretion of IL-1β into extracellular medium, and total levels of IL-1β and pro-IL-1β in cell lysates were determined using ELISA kit.

2.6. Construction and characterization of pVAX1-IA

The coding sequence of IL-1Ra (GeneBank accession no. NM_173842.2) and ApoAI (GeneBank accession no. X07496) were subcloned into the eukaryotic expression vector pVAX1 with HindIII, BamHI and XhoI sites to construct pVAX1-IL-1Ra and pVAX1-IA, respectively. A linker (GGGGS) was introduced between IL-1Ra and ApoAI for flexibility. Top 10 competent cells (V209, novoprotein, China) were applied for transformation.

For *in vitro* expression assay, HEK-293T (2×10^6 cells/well in 6-well plates) was transfected with 5 μg of pVAX1 or pVAX1-IA using lipofectamine 2000. The cell lysates and supernatant were harvested at 24 h post transfection for assessing the expression of IL-1Ra-ApoAI fusion protein by ELISA. The location of IL-1Ra-ApoAI in cells was observed by confocal microscope. Mice were received intramuscular injections (50 μg of pVAX1-IL-1Ra or pVAX1-IA) to assess the expression levels of IL-1Ra *in vivo*.

The IL-1β antagonizing activity of pVAX1-IA was assessed by previously reported method [23]. A549 (5×10^4 cells/well in 96-well plates) was seeded and allowed to grow overnight. Culture media was removed on the following day and treated with pVAX1-IA-transfected HEK-293T cell supernatant (IL-1Ra, 6.4 ng/ml) for 1 h, and then stimulated with recombinant human IL-1β (100 pg/ml) for 6 h. The concentration of IL-6 in A549 cell supernatant was detected using ELISA.

2.7. Synthesis of DSPE-PEG-Galactose and DSPE-PEG

A total of 15 mg DSPE was dissolved in chloroform, to which 170 mg of

Galactose-PEG-NHS or PEG-NHS was added and followed by 80 μL of triethylamine (Nt_3N) (the molar ratio of Galactose-PEG-NHS/PEG-NHS to DSPE was about 3:1). The reaction was continuously stirred at room temperature for 24 h. After removing chloroform by rotary evaporation, the condensed mixture was redissolved in N, N-dimethylformamide, dialyzed against deionized water for 24 h and freeze-dried. The synthesized DSPE-PEG-Galactose was analyzed by HNMR spectrometer (Ascend 600 MHz, Bruker, Germany) and MALDI-TOF mass spectrum (AB SCIEX, USA).

2.8. Preparation of lipo-pVAX1-IA, Plipo-pVAX1-IA and Glipo-pVAX1-IA nanobiologics

DOTAP/cholesterol liposomes were produced using the thin film hydration method [29]. Plasmid pVAX1-IA was incubated with DOTAP/cholesterol liposomes for 30 min at room temperature to obtain lipo-pVAX1-IA. Lipo-pVAX1-IA was further PEGylated using a post-insertional reaction by adding DSPE-PEG or DSPE-PEG-Galactose (1 mol% of total lipids) [33,34]. Afterwards, the targeted Glipo-pVAX1-IA (DSPE-PEG-Galactose-modified lipo-pVAX1-IA) and Plipo-pVAX1-IA (DSPE-PEG-modified lipo-pVAX1-IA) were achieved at 50°C for 15 min. Nanobiologic size, surface charge and polydisperse index value (PDI) were determined by a dynamic light scattering (DLS) detector (Malvern, Worcestershire, UK). The morphology of Glipo-pVAX1-IA was observed using transmission electron microscopy.

2.9. Gel retardation assay

The weight/weight ratios between DOTAP/cholesterol liposome and pVAX1-IA were set from 0:1 to 28:1. The lipo/pVAX1-IA was post-inserted with DSPE-PEG-Galactose and loaded onto 1% agarose gel containing Golden Viewer staining. After electrophoresis (90 V for 30 min), the gel was visualized with Chemi-Docimage analyzer (Bio-Rad, Hercules, USA), and the quantification of DNA bands was obtained by Image J software.

The stability of Glipo-pVAX1-IA in serum was also analyzed by agarose gel electrophoresis. Naked pVAX1-IA and Glipo-pVAX1-IA were mixed with fetal bovine serum (FBS) at a ratio of 1:1 (volume/volume). The resulting mixtures were incubated at 37°C for various time points and analyzed by agarose gel electrophoresis.

2.10. *In vitro* cellular uptake and transfection assay

HepG2 cells and Huh7 cells were incubated with lipo-pVAX1-IA, Plipo-pVAX1-IA and Glipo-pVAX1-IA (pVAX1-IA at a weight of 5 μg, labeled with TOTO-3) at 37°C for 3 h and the cellular uptake was assessed by flow cytometry. For the observation of intracellular trafficking, HepG2 cells and Huh7 cells were incubated with Glipo-pVAX1-IA for various time points. After removal of nanobiologics, the cells were co-stained with Hoechst 33342 and lyso-tracker green at 37°C for 30 min for observation using confocal microscope.

HepG2 cells and Huh7 cells were also transfected with galactose-modified Glipo- pCMV-EGFP nanobiologics for 48 h and the fluorescence expression of EGFP was captured using confocal microscope.

2.11. *In vivo* distribution of Glipo-pVAX1-IA

A total of 50 μg of TOTO-3-labeled pVAX1-IA in lipo-pVAX1-IA, Plipo-pVAX1-IA or Glipo-pVAX1-IA was intravenously injected to mice. At 12 h, 24 h and 36 h post injection, the distribution in major organs was quantitatively visualized by IVIS imaging system (PerkinElmer, Waltham, USA).

To detect the sub-organ biodistribution of Glipo-pVAX1-IA, parenchymal and nonparenchymal liver cells were harvested to determine the levels of IL-1Ra at 1, 2 and 3 days post injection. Kupffer cells were labeled with F4/80 for flow cytometry analysis.

2.12. Toxicity and pathology studies

One, seven and fourteen days after mice were intravenously injected with PBS (Control group), blank Glipo and Glipo-pVAX1-IA, samples were separated from mice. Hepatic and kidney damage were analyzed by assessing serum levels of serum aminotransferase (ALT), aspartate transaminase (AST), blood urea nitrogen (BUN) and creatinine. Serum IL-1β, TNF-α and interferon-γ (IFN-γ) were also determined by ELISA. The major organs, including heart, liver, spleen, lung, kidney and brain were obtained and fixed for H&E staining. Images were captured using a light microscope with 200× magnification.

2.13. Statistical analysis

Statistical analyses were performed using GraphPad Prism software. Statistical significance (*$p < 0.05$, **$p < 0.05$) was determined using student's *t* test. Results were represented as mean ± SD.

3. Results

3.1. GSDMD membrane pores were critical for the hypersecretion of IL-1β from chronic ethanol-stimulated macrophages

Recent progress has shown that long-term ethanol treatment amplifies the release of IL-1β from NLRP3-activated macrophages, but the underlying mechanisms that regulate the release of IL-1β remains unclear [35]. Given that IL-1β is not secreted through the conventional ER-Golgi route-mediated protein secretion, we explored whether GSDMD was involved in regulation of IL-1β hypersecretion triggered by chronic ethanol. BMDMs isolated from WT and *GSDMD*$^{-/-}$ mice were incubated with ethanol, followed by challenging with LPS and ATP to activate NLRP3 inflammasome in ethanol-free media. We found that IL-1β levels in cell supernatants of both WT BMDMs and *GSDMD*$^{-/-}$ BMDMs elevated in a dose-dependent manner by chronic ethanol treatment, while ethanol-induced IL-1β hypersecretion significantly diminished in *GSDMD*$^{-/-}$ BMDMs (**Fig. 1A**). Lower amounts of IL-1β secretion in *GSDMD*$^{-/-}$ BMDMs were corresponding to higher amounts of intracellular IL-1β retention, implying the critical role of GSDMD membrane pore in IL-1β hypersecretion from chronic ethanol-exposed macrophages (**Fig. 1B and C**). Given that the blood ethanol concentrations can come up to 100 mM during heavy drinking, this level was perceived to be appropriate for modeling severe human alcoholism [35].

GSDMD membrane pores on pyroptotic cells permit the passage of IL-1β, and also allow the uptake of membrane-impermanent fluorescent dye propidium iodide

(PI) [14]. As shown in **Fig. 1D and E**, caspase-1 and PI double-positive cells significantly increased. In contrast, the percentage of caspase-1 and PI double-positive cells fallen from 45.8% in WT BMDMs to 27.9% in *GSDMD*$^{-/-}$ BMDMs under the exposure of 200 mM ethanol, LPS and ATP, correspondingly the caspase-1-positive but PI-negative cells increased from 7.5% to 23.3%, indicating the causal effects of GSDMD membrane pore in the regulation of membrane permeabilization and IL-1β hypersecretion under the exposure of long-term ethanol.

Acetaldehyde, the toxic metabolite of ethanol, is known to be important to the pathogenesis of ALD [36]. Similar to ethanol, we found that acetaldehyde also triggered the hypersecretion of IL-1β after treatment of LPS and ATP in both WT and *GSDMD*$^{-/-}$BMDMs, while GSDMD membrane pore deletion resulted in more intracellular IL-1β retention in *GSDMD*$^{-/-}$ BMDMs as compared to WT BMDMs (**Fig. 1F and G**). Taken together, our results demonstrated that GSDMD membrane pore was essential for IL-1β hypersecretion in response to chronic ethanol or acetaldehyde exposure.

3.2. Deletion of GSDMD decreased IL-1β release and attenuated alcoholic steatohepatitis

Given the importance of GSDMD membrane pore in IL-1β release from ethanol or acetaldehyde-exposed BMDMs that was observed *in vitro* studies, we next explored the role of GSDMD in murine model of ASH by chronic-binge ethanol feeding on WT and *GSDMD*$^{-/-}$ mice. Upregulated levels of serum ALT and liver triglyceride (TG), as well as increased number and size of vacuoles in H&E staining

were observed in WT mice after the treatment of chronic-binge ethanol (**Fig. 2A and B**). In contrast, *GSDMD*$^{-/-}$ mice presented lower levels of serum ALT and liver TG, and attenuated hepatocellular damage and lipid storage in liver after ethanol feeding. Consistent with the decreased IL-1β secretion in chronic ethanol-exposed *GSDMD*$^{-/-}$ BMDMs, serum levels of IL-1β also decreased in *GSDMD*$^{-/-}$ mice compared with WT mice (**Fig. 2C**). Meanwhile, the levels of IL-1β in liver also reduced in *GSDMD*$^{-/-}$ mice, which may be associated with the reduced systemic inflammation and hepatocellular damage by GSDMD deficiency.

Notably, the expression of GSDMD and IL-1β upregulated in both hepatocytes and nonparenchymal liver cells, whereas nonparenchymal liver cells were recognized as the primary cells for elevated GSDMD and IL-1β (**Fig. 2D**). Using fluorescent immunohistochemistry analysis, we observed that the intense GSDMD expression (green), displaying a “ring of fire”, concentrated at F4/80-positive kupffer cells (yellow) after alcohol feeding, confirming the higher expression of GSDMD in nonparenchymal liver cells than hepatocytes (**Fig. 2E**). In addition, IL-1β (red) was mostly released into extracellular space without co-localization with GSDMD and F4/80 in WT livers (overlap appeared red), whereas the majority of IL-1β was retained inside the F4/80-positive cells of the liver of *GSDMD*$^{-/-}$ mice (merge appeared orange). The robust retention of IL-1β in the kupffer cells of *GSDMD*$^{-/-}$ mice further underscored the key role of GSDMD in pathogenic release of IL-1β in ASH.

3.3. Development of Glipo-pVAX1-IA nanobiologics for hepatocyte-targeted delivery of IL-1Ra

Inspired by above observations that IL-1β release exerted strong proinflammatory effects to promote the pathogenesis of ASH, IL-1Ra was employed and modified to block IL-1β inflammatory responses. To prolong the half-life and improve liver accumulation of IL-1Ra, we took advantage of ApoAI as the targeting and stabilizing moiety to construct the therapeutic plasmid pVAX1-IA that expressed the fusion protein IL-1Ra-ApoAI (**Fig. 3A**). The expression was determined by strong specific bands of IL-1Ra-ApoAI (IL-1Ra-ApoAI, 48 kDa; IL-1Ra, 20 kDa; ApoAI, 28 kDa) in pVAX1-IA-transfected HEK-293T cells (**Fig. 3B**). The obvious signals of ApoAI in immunofluorescence analysis and upregulated levels of IL-1Ra in the supernatant of pVAX1-IA-transfected HEK-293T cells verified the efficient expression and secretion of IL-1Ra-ApoAI (**Fig. 3C and Supplementary Fig. 1A**). The IL-1β antagonizing activity of pVAX1-IA was assessed using an established *in vitro* model, where interleukin-6 (IL-6) was produced by IL-1β stimulation in A549 cells. Compared to pVAX1 group, significantly less IL-1β-induced IL-6 production was shown in A549 cells treated with pVAX1-IA-transfected HEK-293T cell supernatant (**Supplementary Fig. 1B**). This suggested that HEK-293T cell-secreted IL-1Ra was able to block IL-1β and suppress its downstream signaling pathway. Next, mice were intramuscular injected with pVAX1-IA and pVAX1-IL-1Ra to detect the *in vivo* expression of IL-1Ra-ApoAI. As shown in **Fig. 3D**, mice that were treated with pVAX1-IA displayed a higher level of IL-1Ra in liver tissues with a prolonged duration than pVAX1-IL-1Ra.

In addition, galactose modified nanobiologics (Glipo-pVAX1-IA) were

introduced for hepatocyte-specific expression of IL-1Ra (**Fig. 3F**). As shown in **Fig. 3E**, the lipid DSPE was functionalized with galactose via a PEG spacer to form DSPE-PEG-Galactose, in which long PEG spacer was anticipated to reduce the toxicity and prolong the duration of cationic liposomes [32]. HNMR spectrometer and MALDI-TOF mass spectrum validated the high purity and conjugation of DSPE-PEG-Galactose (**Supplementary Fig. 2A-D**). The synthesized DSPE-PEG-Galactose was post-inserted into the lipid bilayer of lipo-pVAX1-IA to facilitate hepatocyte-targeted delivery of therapeutic IL-1Ra.

To optimize the delivery efficacy of Glipo-pVAX1-IA, gel retardation, size and zeta potential analysis as well as IL-1Ra expression assay were applied to screen the appropriate weight ratio between blank cationic liposomes (DOTAP/cholesterol) and pVAX1-IA. The electrophoresis results determined that pVAX1-IA was fully encapsulated at a weight ratio of 8 or beyond, which was evidenced by no bright band of free pVAX1-IA at 4215 bp (**Fig. 3G)**. Obviously, the ratio of 20:1 between liposome and DNA contributed to the highest IL-1Ra expression among all examined DNA/liposomes ratios (**Fig. 3H)**. DLS analysis determined that the mean hydrodynamic diameter of the nanobiologics at the ratio of 20:1 was 155 nm, with a zeta-potential of 18.7 mV (**Supplementary Fig. 2E-G)**. Transmission electron microscopy revealed the spherical morphology of the nanobiologics (**Fig. 3I)**. Accordingly, the weight ratio of 20:1 was chosen as the optimal ratio to develop Glipo-pVAX1-IA.

Another important requirement for successfully gene delivery is the stability in

serum. Naked pVAX1-IA was completely fragmented upon treatment with FBS for 10 min, as evidenced by the disappearance of the pVAX1-IA band at 4215 bp after gel electrophoresis (**Fig. 3J)**. By contrast, DNA that was encapsulated into Glipo-pVAX1-IA preserved the integrity even at 12 h, demonstrating the fine stability of the nanobiologics to protect the gene cargo from enzymatic degradation in serum.

3.4. Glipo-pVAX1-IA nanobiologics displayed excellent hepatocellular uptake and gene expression *in vitro*

Efficient cellular uptake and endosomal escape of Glipo-pVAX1-IA nanobiologics are critical for successful expression of the fusion protein IL-1Ra-ApoAI. The plasmid pVAX1-IA was marked with TOTO-3 to observe the internalization of nanobiologics in primary mouse hepatocytes and two hepatic cell lines HepG2 and Huh7 cells by flow cytometry. Glipo-pVAX1-IA displayed significantly higher intracellular fluorescence intensity of TOTO-3-labled pVAX1-IA than lipo-pVAX1-IA and Plipo-pVAX1-IA (lipo-pVAX1-IA was post-inserted DSPE-PEG to obtain Plipo-pVAX1-IA), suggesting that galactose modification promoted high hepatocellular uptake (**Fig. 4A and B, Supplementary Fig. 3A and B**).

To investigate whether Glipo-pVAX1-IA could efficiently escape from endosomes, confocal microscopy was performed to observe the intracellular trafficking of Glipo-pVAX1-IA in HepG2 and Huh7 cells. Based on the results show in **Supplementary Fig. 3C and D**, Glipo-pVAX1-IA adhered to cell membranes at 0.5 h. After incubation for 1 h, the nanobiologics initially entered into cells and

co-localized with the endosome, as exhibited by organ spots in the merged images. Whereas at 4 h, separated pVAX1-IA (red) and lyso-tracker (green) were obviously observed, indicating the successful release of pVAX1-IA from endosomes. Furthermore, a strong expression of EGFP was observed in cells that were exposed to Glipo-pCMV-EGFP in HepG2 and Huh7 cells at 48 h post transfection **(Supplementary Fig. 3E and F)**. Similar results were observed in the primary mouse hepatocytes, confirming that Glipo-pVAX1-IA nanobiologics enabled excellent internalization and endosomal escape for hepatocellular gene expression *in vitro* (**Fig. 4C and D**).

3.5. Glipo-pVAX1-IA nanobiologics specifically targeted hepatocytes in vivo and induced a local and prolonged expression of IL-1Ra

Motivated by the favorable hepatocyte uptake *in vitro*, we next evaluated hepatocyte-targeting specificity of Glipo-pVAX1-IA *in vivo*. Glipo-pVAX1-IA, Plipo-pVAX1-IA and lipo-pVAX1-IA labeled with TOTO-3 were intravenous injected into mice. The *in vivo* distribution of various organs was visualized by IVIS spectrum imaging analysis after administration for indicated time points. As expected, the fluorescence images of isolated *ex vivo* organs showed that Glipo-pVAX1-IA was rapidly captured by liver tissues within 12 h, and displayed the brightest signals at 24 h post injection, indicating the liver tropism of galactose-functioned nanobiologics (**Fig. 5A and B)**. Importantly, the fluorescence intensity in Glipo-pVAX1-IA group persisted for at least 36 h. Compared to Glipo-pVAX1-IA, administration of lipo-pVAX1-IA resulted in a high accumulation in lung tissues, which may be

attributed to the entrapment of cationic liposomes by lung vascular tree. Additionally, obvious accumulation of TOTO-3-pVAX1-IA in kidney tissues was observed in Plipo-pVAX1-IA group possibly due to the passive uptake by reticuloendothelial system.

To obtain detailed insight into the sub-organ biodistribution of Glipo-pVAX1-IA, we examined the TOTO-3-labled pVAX1-IA in isolated hepatocytes and kupffer cells after injection for 12 h. We observed a predominant internalization of pVAX1-IA in hepatocytes and a minimal uptake by kupffer cells in Glipo-pVAX1-IA group by flow cytometry (**Fig. 5C**). In contrast, Plipo-pVAX1-IA exhibited higher uptake by kupffer cells but lower uptake by hepatocytes. The preferential hepatocyte-targeting of Glipo-pVAX1-IA was further confirmed by the strong and prolonged expression of IL-1Ra in the isolated primary hepatocytes (**Fig. 5D**). Overall, these results suggested that Glipo-pVAX1-IA efficiently delivered pVAX1-IA into hepatocytes and achieved significant expression of IL-1Ra, potentially implying the local and prolonged therapeutics effects of Glipo-pVAX1-IA in the liver.

3.6. Glipo-pVAX1-IA nanobiologics protected against hepatic inflammatory cells infiltration and liver damage triggered by alcohol feeding

Above findings promoted us to validate whether Glipo-pVAX1-IA was a potential therapeutic approach for ASH. We next assessed the *in vivo* efficacy of Glipo-pVAX1-IA, compared with PBS (control group), free pVAX1-IA, lipo-pVAX1-IA and Plipo-pVAX1-IA with the chronic-binge alcohol consumption model. This model that is similar to patients with alcoholism who have a history of

long-term drinking and a recent excessive alcohol consumption, has been applied for the therapeutic efficacy evaluation of IL-1Ra *in vivo* [11]. As shown in **Fig. 6A-B**, mice receiving Glipo-pVAX1-IA displayed outstanding therapeutic outcomes with lowest levels of serum ALT, liver TG, serum and liver IL-1β, followed by Plipo-pVAX1-IA and lipo-pVAX1-IA. Contrary to Glipo-pVAX1-IA, serum ALT and liver TG levels have no reduction in the free pVAX1-IA group due to the instability of naked pVAX1-IA in serum (**Fig. 3I**). Histological examination and Oil-O-Red staining further confirmed attenuated liver steatosis and damage in Glipo-pVAX1-IA groups (**Fig. 6C**). The higher therapeutic efficacy of Glipo-pVAX1-IA over lipo-pVAX1-IA and Plipo-pVAX1-IA should be attributed to its hepatocytes-targeting specificity and consequently sustained release of therapeutic IL-1Ra in liver tissues.

IL-1Ra is a well-known to block the effects of IL-1β in recruiting immune cells and amplifying inflammatory responses [17]. Next we addressed whether the suppressed inflammatory cells recruitment was involved in the potent therapeutic efficacy of Glipo-pVAX1-IA nanobiologics. Immunohistochemical analysis of mice after chronic-binge alcohol consumption revealed that Gr-1-positive neutrophils and F4/80-positive macrophages aggregated in liver tissues, but returned to basal levels by Glipo-pVAX1-IA treatment (**Supplementary Fig. 4A-C**). In addition, IL-17A concentrations in serum and liver tissue also strongly decreased, indicating the potential suppressive impact of Glipo-pVAX1-IA on Th17 cells (**Fig. 6D**). To further confirm the function of Glipo-pVAX1-IA on Th17 cells, nonparenchymal liver cells were isolated and double-stained with CD4 and IL-17A for flow cytometry analysis.

As expected, the levels of Th17 cells in livers was lowest in Glipo-pVAX1-IA-treated mice. (**Fig. 6E and F**). These results collectively demonstrated that Glipo-pVAX1-IA nanobiologics exerted significant therapeutic benefits on murine ASH in conjunction with reduced hepatic inflammatory responses.

3.7. Administration of Glipo-pVAX1-IA did not cause systemic toxicity in mice

Safety is a key aspect of nanoparticles and should be taken into consideration for clinical applications. We next investigated whether intravenous administration of blank Glipo or Glipo-pVAX1-IA would initiate inflammatory responses and systemic toxicity. Administration of the blank Glipo or Glipo-pVAX1-IA did not cause any significant differences in serum biochemical analysis (ALT, AST, BUN and creatinine) and serum concentrations of cytokines (IFN-γ, TNF-α and IL-1β) at 1, 7 and 14 days post injection (**Fig. 7A and B**). Furthermore, histological analysis confirmed minimal morphological changes in tissue architecture compared to the control group (**Fig. 7C**). All of these observations indicated that both blank Glipo and Glipo-pVAX1-IA were safe delivery vehicles with enhanced transfection efficiency.

4. Discussion

Given the importance of IL-1β in the development of ASH, and IL-1β is secreted through un-conventional protein secretion route, our studies provided compelling evidence for the critical role of GSDMD membrane pore in regulation long-term ethanol-triggered IL-1β hypersecretion from macrophages. The reduced IL-1β release and attenuated alcoholic steatohepatitis in *GSDMD*$^{-/-}$ mice further verified the casual role of GSDMD in pathogenic IL-1β release during ASH. It is known that IL-1β

initiates the downstream inflammatory signaling pathways through binding to IL-1R1, while IL-1Ra functions as a competitor ligand of IL-1R1 and can antagonize the proinflammatory effects of IL-1β [16,17]. The short half-life (4-6 h) of IL-1Ra due to the rapid clearance from kidney encouraged us to optimize the practical applications of IL-1Ra. In the current study, IL-1Ra coding sequence was firstly tethered to ApoAI gene in pVAX1, followed by being encapsulated into galactose-functioned nanobiologics for hepatocyte-specific gene delivery. As expected, the resulting Glipo-pVAX1-IA facilitated local and sustained expression of IL-1Ra in the liver and exerted efficient therapeutic effects against ASH. These results suggested a novel strategy for the hepatocyte-specific and prolonged delivery of IL-1Ra to treat ASH.

IL-1β is well known as a pivotal pathogenic cytokine in various liver diseases, including immune-mediated hepatitis, alcoholic and nonalcoholic steatohepatitis [37-41]. The robust induction of IL-1β in alcoholic steatohepatitis has been demonstrated in mice and patients with ASH. Moreover, mice deficient in the NLRP3, caspase-1, IL-1R1 were rescued from alcohol-triggered hepatic damage and steatosis [7]. These studies confirmed the crucial role of IL-1β in the pathogenesis of ASH, however, it remained unclear whether suppressing IL-1β release into the extracellular space could have the similar therapeutic outcomes for ASH. Inspired by recent studies showing that GSDMD membrane pore is essential for unconventional release of IL-1β, we explored and identified that activated GSDMD formed membrane pores for IL-1β release in the liver of mice suffering from ASH. This finding is consistent with a recent study demonstrating robust activation of GSDMD-mediated pyroptosis in

murine model of ASH, but the regulatory role of GSDMD in IL-1β release during ASH remains to be determined [42]. In our work, we demonstrated that genetic deletion of GSDMD prevented membrane pore formation and excessive IL-1β secretion, thus ameliorating alcohol-induced liver damage. These findings uncovered a novel mechanism regarding the IL-1β release in ASH, and also highlighted the potential of antagonizing IL-1β for the treatment of ASH. Meanwhile, some studies have recently uncovered that slow secretion of IL-1β proceeds by an unconventional pathway that is independent of GSDMD, and GSDMD is only necessary for rapid secretion of IL-1β [43]. It might be accountable for the moderate protection from ASH by GSDMD deficiency in our study, and thus we focused on antagonizing IL-1β by hepatocyte-targeted nanobiologics instead of down-regulating GSDMD by therapeutic strategies.

Antagonizing IL-1β with recombinant IL-1Ra (Anakinra) has been demonstrated to be effective in ASH [7,11]. However, short half-life and detrimental side effects, such as neutropenia and increased risks of infections, come with systemic IL-1Ra administration, thus leading to limited clinical applications [18]. Our objective was to construct a fusion molecular that could both prolong the circulation of IL-1Ra and allow it to block IL-1β predominately in the liver instead of systemic suppression. Herein, ApoAI was fused at the C-terminal of IL-1Ra in FDA-authorized eukaryotic plasmid pVAX1. Indeed, the novel fusion molecular pVAX1-IA was far superior to pVAX1-IL-1Ra, as evidenced by a higher level of IL-1Ra in the liver following intramuscular injection, which shed light on a novel modification of IL-1Ra for the

treatment of liver diseases. This finding was consistent with our previous study showing that tethering interleukin-22 to ApoAI contributed to efficient liver targeting, further confirming the liver targeting potential of ApoAI [29,44].

Cationic liposomes-based nanobiologics are an attractive strategy in the gene delivery because of their large payload and strong efficacy in enhancing cellular uptake [45,46]. However, the transformative potential of conventional cationic liposomes has been impended by several drawbacks, such as short duration and non-tissue selectivity [47]. To overcome these barriers, investigations to modify cationic liposomes with targeting ligands have been conducted [48,49]. For hepatocellular targeting, sugars such as N-acetylgalactosamine and galactose were introduced for active targeting via binding with ASGPR [30-32]. In agreement with these studies, our data showed that galactose-functioned nanobiologics were specifically internalized into hepatocytes. In addition, Glipo-pVAX1-IA displayed efficient escape of therapeutic genes from lysosomal compartments. It might be explained that cationic liposomes-mediated ion-pair formation triggered the disruption of endosomal membrane [50]. Most importantly, Glipo-pVAX1-IA presented a remarkable therapeutic outcomes on ASH, as indicated by decreased serum ALT and liver TG, as well as improved liver histopathology. However, treatment of lipo-pVAX1-IA or Plipo-pVAX1-IA only led to a moderate decrease of steatohepatitis. These results suggested that administration of Glipo-pVAX1-IA resulted in a high accumulation in the liver, allowing for increased and sustained expression of IL-1Ra to suppress the progress of ASH.

We have demonstrated that Glipo-pVAX1-IA played a protective role in ASH, but the mechanism of its therapeutic effects remains unclear. Several lines of evidence suggested that IL-1β promoted infiltration of neutrophils to liver tissues in response to injury, but the infiltration obviously impaired in IL-1R1 knockout mice [51,52]. Another study confirmed that IL-1β participated in the differentiation of Th17 cells and thereby contributed to the development of liver diseases [53]. Correspondingly, our results suggested that blocking IL-1β by Glipo-pVAX1-IA suppressed the infiltration of macrophages and neutrophils, as well as the production of IL-17A triggered by alcohol consumption *in vivo*, which contributes to the therapeutic benefits on murine ASH.

Glipo-pVAX1-IA nanobiologics and many other nonviral vectors hold therapeutic potential to treat a variety of liver disorders, as they allow the therapeutic nucleic acids to express locally at the disease sites in large quantities, but nontoxic delivery of DNA therapeutics remains a fundamental challenge [54,55]. It is noteworthy that in our investigation there is no obvious cytokine induction and histological injury of major organs in Glipo-pVAX1-IA nanobiologics-treated mice, which might be attributed to the decreased positive charge by the long PEG spacer for galactose and the active hepatocyte-targeting properties. However, the evaluation of our nanobiologics was limited by employing only cell line-based and murine models, and more accurate preclinical animal models that mimic the clinical profile need to be introduced in the future investigation. Furthermore, the more in-depth and systemic investigations by innovative technologies are required for better understanding and

knowing how to modulate them to bring us closer to clinical applications.

5. Conclusions

In summary, we identified the critical role of GSDMD membrane pore in chronic ethanol-triggered IL-1β hypersecretion and developed a novel regimen for the hepatocyte-specific and prolonged delivery of IL-1Ra by utilizing Glipo-pVAX1-IA to treat ASH. Four advantages highlighted the practical applications of this strategy: (i) Galactose functionalization facilitated hepatocyte-specific delivery of the therapeutic gene pVAX1-IA. (ii) Fusion IL-1Ra to ApoAI paved the way for secondary targeting to the liver and prolonged the duration of IL-1Ra. (iii) Glipo-pVAX1-IA prevented the development of ASH via prolonged expression of IL-1Ra in livers. (iv) Our research offered a promising delivery strategy for other therapeutic proteins with short half-life to treat liver diseases.

Author contributions

J.L. and W.C. performed most of the experiments and wrote the paper. J.F., S.W. and X.Z. fabricated characterized nanostructures and mechanical properties. X.J. and W.Z. analyzed the samples after mice model. Y.W., Z.F. and J.Z. analyzed and interpreted data. M.L. and D.J. studied conceptualization, designed experiments, and supervised the whole work.

Data availability

The raw required to reproduce the findings from this study will be made available to interested investigators upon request.

Acknowledgments

This study was supported by National Natural Science Foundation of China (No. 81573332, No.81773620 and No.81803529) and National Key Basic Research Program of China (2015CB931800).

We thank Dr. Feng Shao for sharing *GSDMD*$^{-/-}$ mice.

Competing Interests

The authors have declared that no competing interest exists.

References:

1. World Health Organization. Global status report on alcohol and health. Updated 2014. http://www.who.int/substance_abuse/publications/global_alcohol_report/en/.
2. H.J. Wang, B. Gao, S. Zakhari, L.E. Nagy, Inflammation in alcoholic liver disease, Annu. Rev. Nutr. 32 (2012) 343–368.
3. A. Louvet, P. Mathurin, Alcoholic liver disease: mechanisms of injury and targeted treatment, Nat. Rev. Gastroenterol. Hepatol. 12 (2015) 231–242.
4. L. Abenavoli, N. Milic, S. Rouabhia, G. Addolorato, Pharmacotherapy of acute alcoholic hepatitis in clinical practice, World. J. Gastroenterol. 20 (2014) 2159–

2167.

5. M. Amini, B.A. Runyon, Alcoholic hepatitis 2010: a clinician's guide to diagnosis and therapy, World. J. Gastroenterol. 16 (2010) 4905–4912.
6. G. Szabo, J. Petrasek, Inflammasome activation and function in liver disease, Nat. Rev. Gastroenterol. Hepatol. 12 (2015) 387-400.
7. J. Petrasek, S. Bala, T. Csak, D. Lippai, K. Kodys, V. Menashy, M. Barrieau, S.Y. Min, E.A. Kurt-Jones, G. Szabo, IL-1 receptor antagonist ameliorates inflammasome-dependent alcoholic steatohepatitis in mice, J. Clin. Invest. 122 (2012) 3476-3489.
8. Y. Kamari, A. Shaish, E. Vax, S. Shemesh, M. Kandel-Kfir, Y. Arbel, S. Olteanu, I. Barshack, S. Dotan, E. Voronov, C.A. Dinarello, R.N. Apte, D. Harats, Lack of interleukin-1α or interleukin-1β inhibits transformation of steatosis to steatohepatitis and liver fibrosis in hypercholesterolemic mice, J. Hepatol. 55 (2011) 1086-1094.
9. K. Miura, Y. Kodama, S. Inokuchi, B. Schnabl, T. Aoyama, H. Ohnishi, J.M. Olefsky, D.A. Brenner, E. Seki, Toll-like receptor 9 promotes steatohepatitis by induction of interleukin-1β in mice, Gastroenterology 139 (2010) 323-334.
10. H. Tilg, A.R. Moschen, G. Szabo, Interleukin-1 and inflammasomes in alcoholic liver disease/acute alcoholic hepatitis and nonalcoholic fatty liver disease/nonalcoholic steatohepatitis, Hepatology 64 (2016) 955-965.
11. K. Cui, G. Yan, C. Xu, Y. Chen, J. Wang, R. Zhou, L. Bai, Z. Lian, H. Wei, R. Sun, Z. Tian, Invariant NKT cells promote alcohol-induced steatohepatitis through

interleukin-1β in mice, J. Hepatol. 62 (2015) 1311-1318.

12. G. Lopez-Castejon, D. Brough, Understanding the mechanism of IL-1β secretion, Cytokine. Growth. Factor. Rev. 22 (2011) 189-195.
13. J. Shi, Y. Zhao, K. Wang, X. Shi, Y. Wang, H. Huang, Y. Zhuang, T. Cai, F. Wang, F. Shao, Cleavage of GSDMD by inflammatory caspases determines pyroptotic cell death, Nature 526 (2015), 660-665.
14. C.L. Evavold, J. Ruan, Y. Tan, S. Xia, H. Wu, J.C. Kagan, The Pore-Forming Protein Gasdermin D Regulates Interleukin-1 Secretion from Living Macrophages, Immunity 48 (2018) 35-44.
15. W.T. He, H. Wan, L. Hu, P. Chen, X. Wang, Z. Huang, Z.H.Yang, C.Q. Zhong, J. Han, Gasdermin D is an executor of pyroptosis and required for interleukin-1β secretion, Cell. Res. 25 (2015) 1285-1298.
16. C. Garlanda, C.A. Dinarello, A. Mantovani, The interleukin-1 family: back to the future, Immunity 39 (2013) 1003-1018.
17. C.A. Dinarello, A. Simon, J.W. Van, Treating inflammation by blocking interleukin-1 in a broad spectrum of diseases, Nat. Rev. Drug. Discov. 11 (2012) 633-652.
18. M.S. Akash, K. Rehman, S. Chen, IL-1Ra and its delivery strategies: inserting the association in perspective, Pharm. Res. 30 (2013) 2951-2966.
19. M.S. Akash, Q. Shen, K. Rehman, S. Chen, Interleukin-1 receptor antagonist: a new therapy for type 2 diabetes mellitus, J. Pharm. Sci. 101 (2012) 1647–1658.
20. P. Yu, C. Zheng, J. Chen, G. Zhang, Y. Liu, X. Suo, G. Zhang, Z. Su, Investigation

on PEGylation strategy of recombinant human interleukin-1 receptor antagonist, Bioorg. Med. Chem. 15 (2007) 5396–5405.

21. M.F. Shamji, H. Betre, V.B. Kraus, J. Chen, A. Chilkoti, R. Pichika, K. Masuda, L.A. Setton, Development and characterization of a fusion protein between thermally responsive elastin-like polypeptide and interleukin-1 receptor antagonist: sustained release of a local anti-inflammatory therapeutic, Arthritis. Rheum. 56 (2007) 3650-3661.
22. M. Maes, C. Song, R. Yirmiya, Targeting IL-1 in depression, Expert. Opin. Ther. Targets. 16 (2012) 1097-1112.
23. P. Rider, Y. Carmi, R. Yossef, O. Guttman, H. Eini, T. Azam, C.A. Dinarello, E.C. Lewis, IL-1 Receptor Antagonist Chimeric Protein: Context-Specific and Inflammation-Restricted Activation, J. Immunol. 195 (2015) 1705-1712.
24. S. Acton, A. Rigotti, K.T. Landschulz, S. Xu, H.H. Hobbs, M. Krieger, Identification of scavenger receptor SR-BI as a high density lipoprotein receptor, Science 271 (1996) 518–520.
25. M.A. Connelly, D.L. Williams, Scavenger receptor BI: a scavenger receptor with a mission to transport high density lipoprotein lipids, Curr. Opin. Lipidol. 15 (2004) 287–295.
26. S.I. Kim, D. Shin, T.H. Choi, J.C. Lee, G.J. Cheon, K.Y. Kim, M. Park, M. Kim, Systemic and specific delivery of small interfering RNAs to the liver mediated by apolipoprotein A-I, Mol. Ther. 15 (2007) 1145–1152.
27. J. Fioravanti, I. González, J. Medina-Echeverz, E. Larrea, N. Ardaiz, G.

González-Aseguinolaza, J. Prieto, P. Berraondo, Anchoring interferon alpha to apolipoprotein A-I reduces hematological toxicity while enhancing immunostimulatory properties, Hepatology 53 (2011) 1864-1873.

28. M.C. Ochoa, J. Fioravanti, I. Rodriguez, S. Hervas-Stubbs, A. Azpilikueta, G. Mazzolini, A. Gúrpide, J. Prieto, J. Pardo, P. Berraondo, I. Melero, Antitumor immunotherapeutic and toxic properties of an HDL-conjugated chimeric IL-15 fusion protein, Cancer. Res. 73 (2013) 139-149.
29. W. Chen, X. Zhang, J. Fan, W. Zai, J. Luan, Y. Li, S. Wang, Q. Chen, Y. Wang, Y. Liang, D. Ju, Tethering interleukin-22 to apolipoprotein A-I ameliorates mice from acetaminophen-induced liver injury, Theranostics 7 (2017) 4135-4148.
30. X.Q. Zhang, X.L.Wang, P.C. Zhang, Z.L. Liu, R.X. Zhuo, H.Q. Mao, K.W. Leong, Galactosylated ternary DNA/polyphosphoramidate nanoparticles mediate high gene transfection efficiency in hepatocytes, J. Control. Release. 102 (2005) 749–763.
31. Y. Hu, M.T. Haynes, Y. Wang, F. Liu, L. Huang, A highly efficient synthetic vector: nonhydrodynamic delivery of DNA to hepatocyte nuclei in vivo, ACS. Nano. 7 (2013) 5376-5384.
32. H. He, M.G.3rd2. Lancina, J. Wang, W.J. Korzun, H. Yang, S. Ghosh, Bolstering cholesteryl ester hydrolysis in liver: A hepatocyte-targeting gene delivery strategy for potential alleviation of atherosclerosis, Biomaterials 130 (2017) 1-13.
33. L.Y. Gao, X.Y. Liu, C.J. Chen, J.C. Wang, Q. Feng, M.Z. Yu, X.F. Ma, X.W. Pei, Y.J. Niu, C. Qiu, W.H. Pang, Q. Zhang, Core-shell type lipid/rPAA-Chol polymer

hybrid nanoparticles for in vivo siRNA delivery, Biomaterials 35 (2014) 2066-2078.

34. Y. Zhao, W. Wang, S. Guo, Y. Wang, L. Miao, Y. Xiong, L. Huang, PolyMetformin combines carrier and anticancer activities for in vivo siRNA delivery, Nat. Commun. 7 (2016) 1182.
35. L.R. Hoyt, M.J. Randall, J.L. Ather, D.P. DePuccio, C.C. Landry, X. Qian, Y.M. Janssen-Heininger, A. van der Vliet, A.E. Dixon, E. Amiel, M.E. Poynter, Mitochondrial ROS induced by chronic ethanol exposure promote hyper-activation of the NLRP3 inflammasome, Redox. Biol. 12 (2017) 883-896.
36. K. Walsh, G. Alexander, Alcoholic liver disease, Postgrad. Med. J. 76 (2000) 280-286.
37. A. Wree, A. Eguchi, M.D. McGeough, C.A. Pena, C.D. Johnson, A. Canbay, H.M. Hoffman, A.E. Feldstein, NLRP3 inflammasome activation results in hepatocyte pyroptosis, liver inflammation, and fibrosis in mice, Hepatology 59 (2014) 898-910.
38. J. Luan, X. Zhang, S. Wang, Y. Li, J. Fan, W. Chen, W. Zai, S. Wang, Y. Wang, M. Chen, G. Meng, D. Ju, NOD-like receptor protein 3 inflammasome-dependent IL-1β accelerated conA-induced hepatitis, Front. Immunol. 9 (2018) 758.
39. X. Zhang, J. Luan, W. Chen, J. Fan, Y. Nan, Y. Wang, Y. Liang, G. Meng, D. Ju, Mesoporous silica nanoparticles induced hepatotoxicity via NLRP3 inflammasome activation and caspase-1-dependent pyroptosis, Nanoscale 10 (2018) 9141-9152.

40. H. Tsutsui, X. Cai, S. Hayashi, Interleukin-1 Family Cytokines in Liver Diseases, Mediators. Inflamm. 157 (2015) 1013-1022.

41. J. Luan, D. Ju, Inflammasome: A Double-Edged Sword in Liver Diseases, Front. Immunol. 9 (2018) 2201.

42. E. Khanova, R. Wu, W. Wang, R. Yan, Y. Chen, S.W. French, C. Llorente, S.Q. Pan, Q. Yang, Y. Li, R. Lazaro, C. Ansong, R.D. Smith, R. Bataller, T. Morgan, B. Schnabl, H. Tsukamoto, Pyroptosis by caspase11/4-gasdermin-D pathway in alcoholic hepatitis in mice and patients, Hepatology 67 (2018) 1737-1753.

43. M. Monteleone, A.C. Stanley, K.W. Chen, D.L. Brown, J.S. Bezbradica, J.B. von Pein, C.L. Holley, D. Boucher, M.R. Shakespear, R. Kapetanovic, V. Rolfes, M.J. Sweet, J.L. Stow, K. Schroder, Interleukin-1b Maturation Triggers Its Relocation to the Plasma Membrane for Gasdermin-D-Dependent and -Independent Secretion, Cell. Rep. 27 (2018) 1425-1433.

44. W. Chen, J. Luan, G. Wei, X. Zhang, J. Fan, W. Zai, S. Wang, Y. Wang, Y. Liang, Y. Nan, C. Yin, Y. Li, M.L. Liu, D. Ju, In vivo hepatocellular expression of interleukin-22 using penetratin-based hybrid nanoparticles as potential anti-hepatitis therapeutics, Biomaterials 187 (2018) 66-80.

45. J.K.L. Wong, R. Mohseni, A.A. Hamidieh, R.E. MacLaren, N. Habib, A.M. Seifalian, Will Nanotechnology Bring New Hope for Gene Delivery? Trends. Biotechnol. 35 (2017) 434-451.

46. R.N. Majzoub, K.K. Ewert, C.R. Safinya, Cationic liposome-nucleic acid nanoparticle assemblies with applications in gene delivery and gene silencing,

Philos. Trans. A. Math. Phys. Eng. Sci. 374 (2016) 20150129.

47. Y. Wang, L. Miao, A. Satterlee, L. Huang, Delivery of oligonucleotides with lipid nanoparticles, Adv. Drug. Deliv. Rev. 87 (2015) 68-80.
48. G.T. Noble, J.F. Stefanick, J.D. Ashley, T. Kiziltepe, B. Bilgicer, Ligand-targeted liposome design: challenges and fundamental considerations. Trends. Biotechnol. 32 (2014) 32-45.
49. R. Van der Meel, L.J. Vehmeijer, R.J. Kok, G. Storm, E.V. van Gaal, Ligand-targeted particulate nanomedicines undergoing clinical evaluation: current status, Adv. Drug. Deliv. Rev. 65 (2013) 1284-1298.
50. D. Simberg, S. Weisman, Y. Talmon, A. Faerman, T. Shoshani, Y. Barenholz, The role of organ vascularization and lipoplex-serum initial contact in intravenous murine lipofection, J. Biol. Chem. 278 (2003) 39858-39865.
51. Y. Koyama, D.A. Brenner, Liver inflammation and fibrosis, J. Clin. Invest. 127 (2017) 55–64.
52. N. Gehrke, N. Hövelmeyer, A. Waisman, B.K. Straub, J. Weinmann-Menke, M.A. Wörns, P.R. Galle, J.M. Schattenberg, Hepatocyte-specific deletion of IL1-RI attenuates liver injury by blocking IL-1 driven autoinflammation, J. Hepatol. 68 (2018) 986-995.
53. Y. Sha, S. Markovic-Plese, A role of IL-1R1 signaling in the differentiation of Th17 cells and the development of autoimmune diseases, Self. Nonself. 2 (2011) 35-42.
54. J. Yoo, S. Choi, K.S. Hwang, W.K. Cho, C.R. Jung, S.T. Kwon, D.S. Im,

Adeno-associated virus-mediated gene transfer of a secreted form of TRAIL inhibits tumor growth and occurrence in an experimental tumor model. J. Gene. Med. 8 (2006) 163–174.

55. L. Miao, Q. Liu, C. Lin, C.M. Luo, Y. Wang, L. Liu, W. Yin, S. Hu, W.Y. Kim, L. Huang, Targeting Tumor-Associated Fibroblasts for Therapeutic Delivery in Desmoplastic Tumors. Cancer. Res. 77 (2017) 719-731.

Figures and figure legends

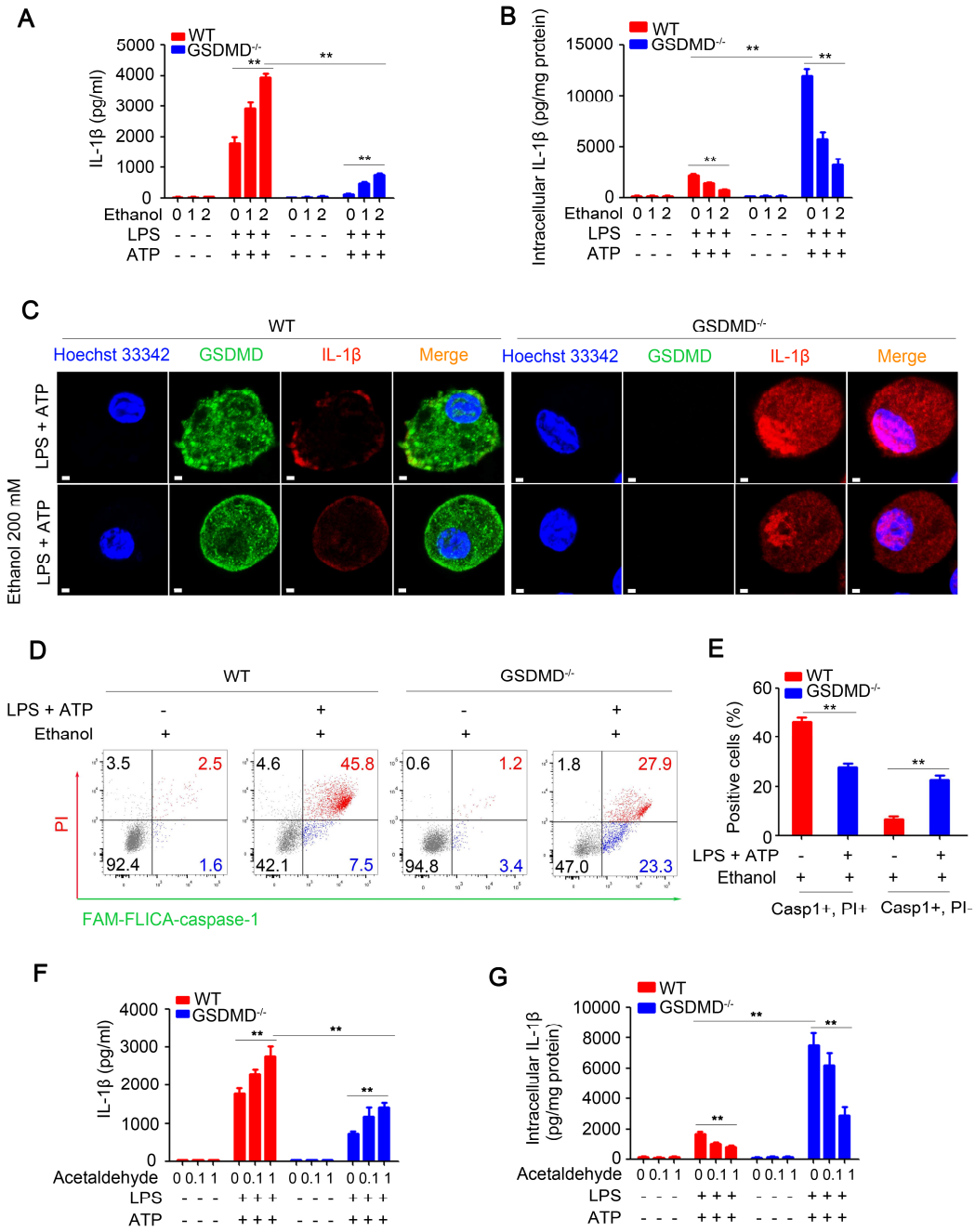

Fig. 1. GSDMD membrane pores were critical for the hypersecretion of IL-1β from chronic ethanol-stimulated macrophages. (**A-E**) WT and *GSDMD*$^{-/-}$ BMDMs were exposed to ethanol (1 and 2 = 100 mM and 200 mM) for 72 h, and then stimulated with or without LPS (100 ng/ml, 5h) and ATP (5 mM, 1 h). (**A**) IL-1β secretion in supernatants was determined by ELISA. (**B**) The levels of IL-1β in the

cell lysates were detected by ELISA. (**C**) Representative immunofluorescence images of GSDMD and IL-1β in BMDMs were presented. Hoechst 33342 (blue), GSDMD (green), IL-1β (red), scale bars = 1.5 μm. (**D**) Membrane pore formation (PI staining) and caspase-1 activation (FAM-FLICA staining) were monitored by flow cytometry. (**E**) Quantitation of caspase-1 and PI double-positive (Casp1+, PI+), and caspase-1-positive but PI-negative (Casp1+, PI-) cells. (**F-G**) WT and *GSDMD*$^{-/-}$ BMDMs were treated with acetaldehyde (0.1 and 1 = 0.1 mM and 1 mM) for 72 h, and then incubated with or without LPS (100 ng/ml, 5 h) and ATP (5 mM, 1 h). Extracellular (**F**) and intracellular (**G**) levels of IL-1β were detected by ELISA. Data indicated means ± SD, n = 3, *$p < 0.05$, **$p < 0.01$.

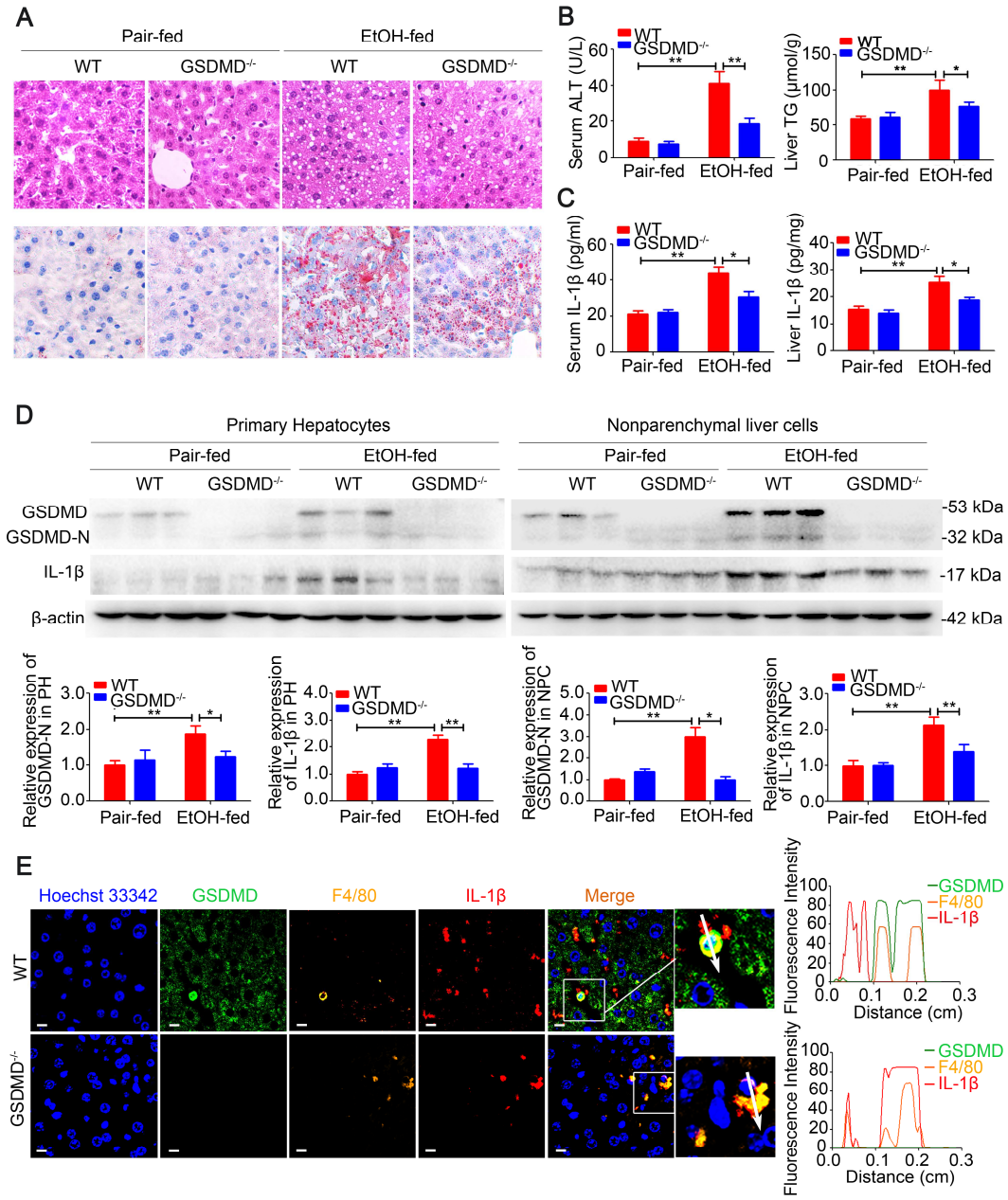

Fig. 2. Deletion of GSDMD decreased IL-1β release and attenuated alcoholic steatohepatitis. WT and *GSDMD*$^{-/-}$ mice were fed with an ethanol (EtOH-fed) or a control (Pair-fed) diet (n = 6 mice per group). (**A**) Hepatocellular damage and steatosis were determined by H&E and Oil-O-Red staining (magnification: 400×). (**B**) Serum ALT and liver TG levels. (**C**) Serum and liver concentrations of IL-1β. (**D**) The protein expression of GSDMD, GSDMD-N and IL-1β in primary hepatocytes (PH) and nonparenchymal liver cells (NPC) were immunoblotted. Densitometric data

were presented after standardization to β-actin. (**E**) Immunofluorescent labeling of GSDMD and IL-1β in macrophages of liver tissues. Hoechst 33342 (blue), GSDMD (green), F4/80 (yellow), IL-1β (red), scale bars = 10 μm. The colocalization of IL-1β with GSDMD and F4/80 were analyzed by Image J. Data indicated means ± SD, n = 3, $*p < 0.05$, $**p < 0.01$.

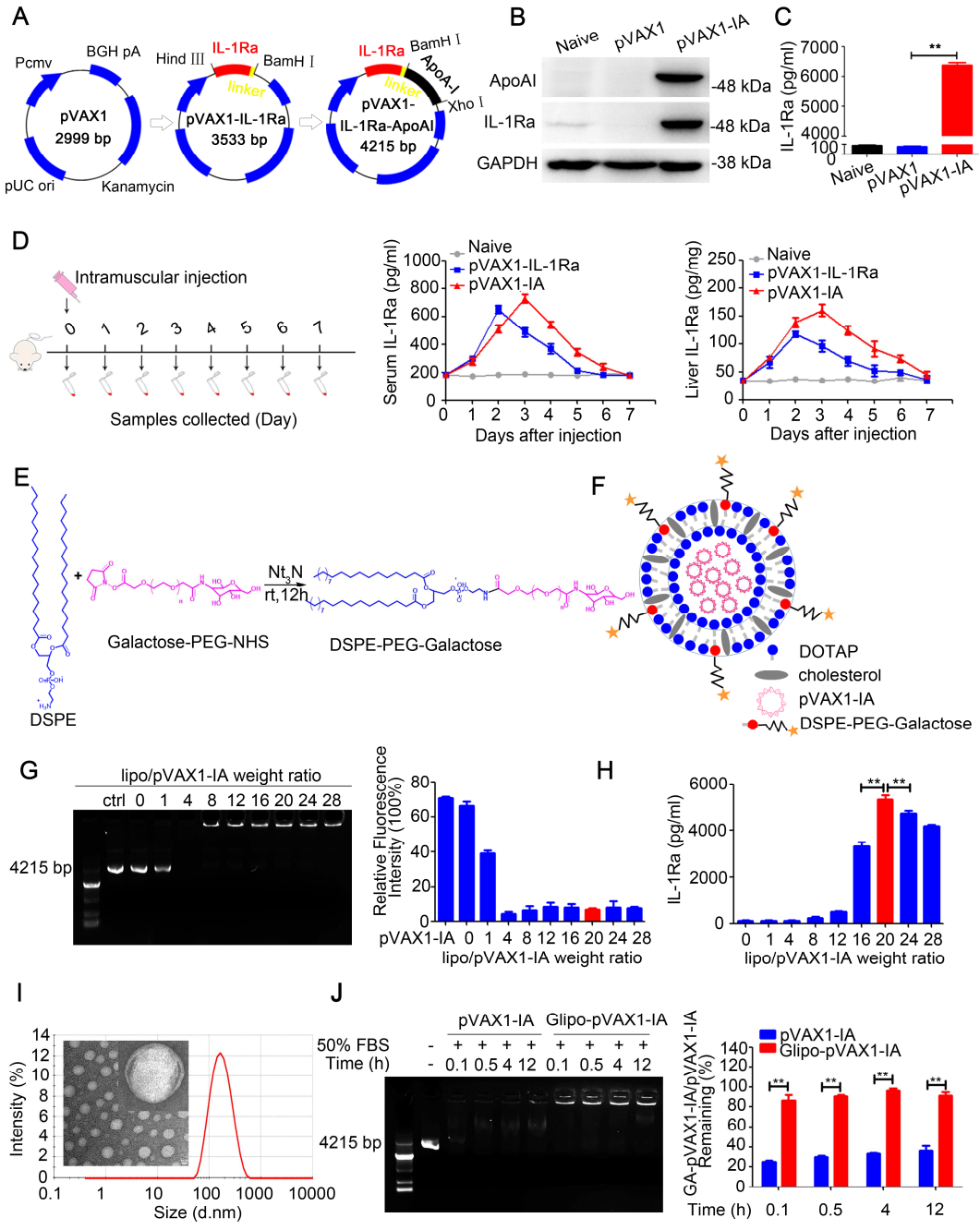

Fig. 3. Development of Glipo-pVAX1-IA nanobiologics for hepatocyte-targeted

delivery of IL-1Ra. (**A**) Schematic diagram of the construction of pVAX1-IL-1Ra and pVAX1-IA plasmid. (**B, C**) HEK-293T cells were transfected with plasmid pVAX1 and pVAX1-IA and the expression of IL-1Ra-ApoAI in cell lysates (**B**) and culture supernatant (**C**) at 24 h post injection were determined using western blot and ELISA, respectively. (**D**) Mice were intramuscularly administrated with PBS (Naïve group), pVAX1 and pVAX1-IA (n = 4 for each group). Serum and liver levels of IL-1Ra at indicated time points post injection were detected by ELISA. (**E**) Synthesis scheme of DSPE-PEG-Galactose. (**F**) Negatively charged pVAX1-IA was condensed by cationic liposomes (DOTAP/cholesterol), followed by post-insertion of DSPE-PEG-Galactose to develop Glipo-pVAX1-IA. (**G**) The complexation capacity of galactose-functioned nanobiologics at various ratios of liposome/DNA was assessed by gel retardation assay. Lane 1: marker; Lane 2: naked pVAX1-IA; Lane 3-11: 5 μg of pVAX1-IA with upregulating weight ratios of liposome. Statistical analysis of gel retardation at various weight ratios. (**H**) The levels of IL-1Ra in cell supernatant of HEK-293T cells at 24 h post transfection. (**I**) Representative images of size distribution and transmission electron microscopy at the ratio of 20:1 (liposome: DNA). (**J**) The stability of Glipo-pVAX1-IA in serum was analyzed by agarose gel electrophoresis. Quantification was obtained. Data indicated means ± SD, n = 3, $*p < 0.05$, $**p < 0.01$.

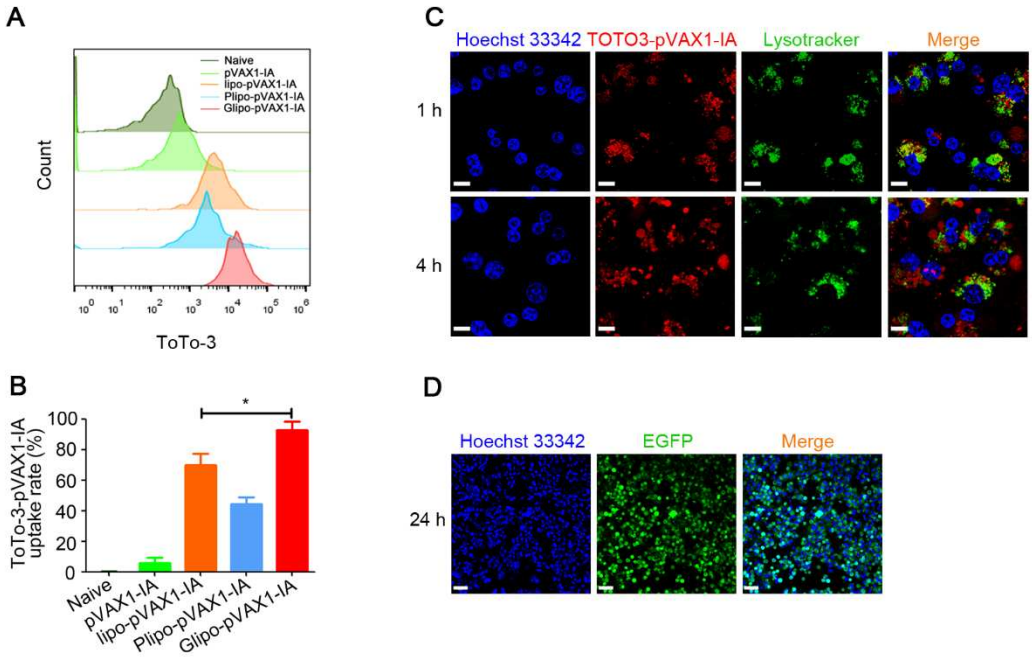

Fig. 4. Glipo-pVAX1-IA nanobiologics displayed excellent hepatocellular uptake and gene expression in the primary mouse hepatocytes. (**A, B**) Fluorescence intensity of TOTO3-labled pVAX1-IA in the primary mouse hepatocytes was detected by flow cytometry after incubation with PBS (Naïve group), free pVAX1-IA, lipo-pVAX1-IA, Plipo-pVAX1-IA and Glipo-pVAX1-IA for 3 h. The quantification was presented in bar graphs. (**C**) Intracellular trafficking of Glipo-pVAX1-IA in the primary mouse hepatocytes was observed by confocal microscopy at 1 h and 4 h. Hoechst 33342 (blue), TOTO-3 (red), lysotracker (green). Scale bars, 10 μm. (**D**) Microscopy analysis of EGFP expression in the primary mouse hepatocytes after transfection for 24 h. Scale bars, 50 μm. Data indicated means ± SD, n = 3, *$p < 0.05$, **$p < 0.01$.

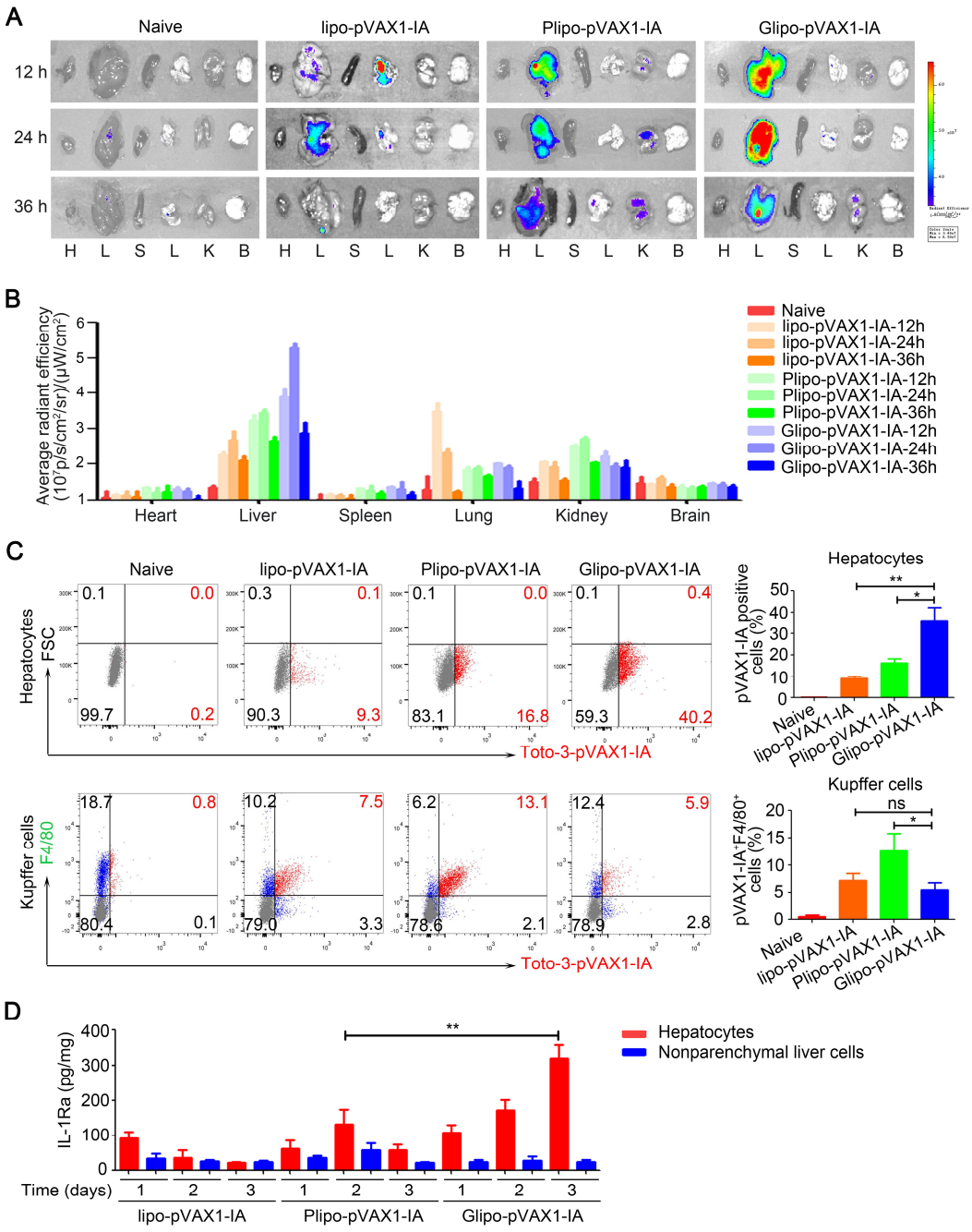

Fig. 5. Glipo-pVAX1-IA nanobiologics specifically targeted hepatocytes *in vivo* and induced a local and prolonged expression of IL-1Ra. C57BL/6 mice were intravenously administrated with PBS (Naive group), lipo-pVAX1-IA, Plipo-pVAX1-IA and Glipo-pVAX1-IA at a single dose of 50 μg pVAX1-IA (n = 4 for each group). (**A**) The fluorescence images of TOTO-3-labled pVAX1-IA in heart, liver, spleen, lung, kidney and brain at 12 h, 24 h and 36 h post intravenous injection were

assessed by IVIS analysis. (**B**) Quantification of the mean fluorescence intensity on each isolated organ. (**C**) Flow cytometry was used to detect TOTO-3-pVAX1-IA in isolated primary hepatocytes and kupffer cells at 12 h post liposomes injection. The quantitative analysis of flow cytometry were presented. (**D**) The levels of IL-1Ra in isolated hepatocytes and nonparenchymal liver cells at 1, 2 and 3 days post nanobiologics injection were analyzed by ELISA. Data indicated means ± SD, *$p < 0.05$, **$p < 0.01$.

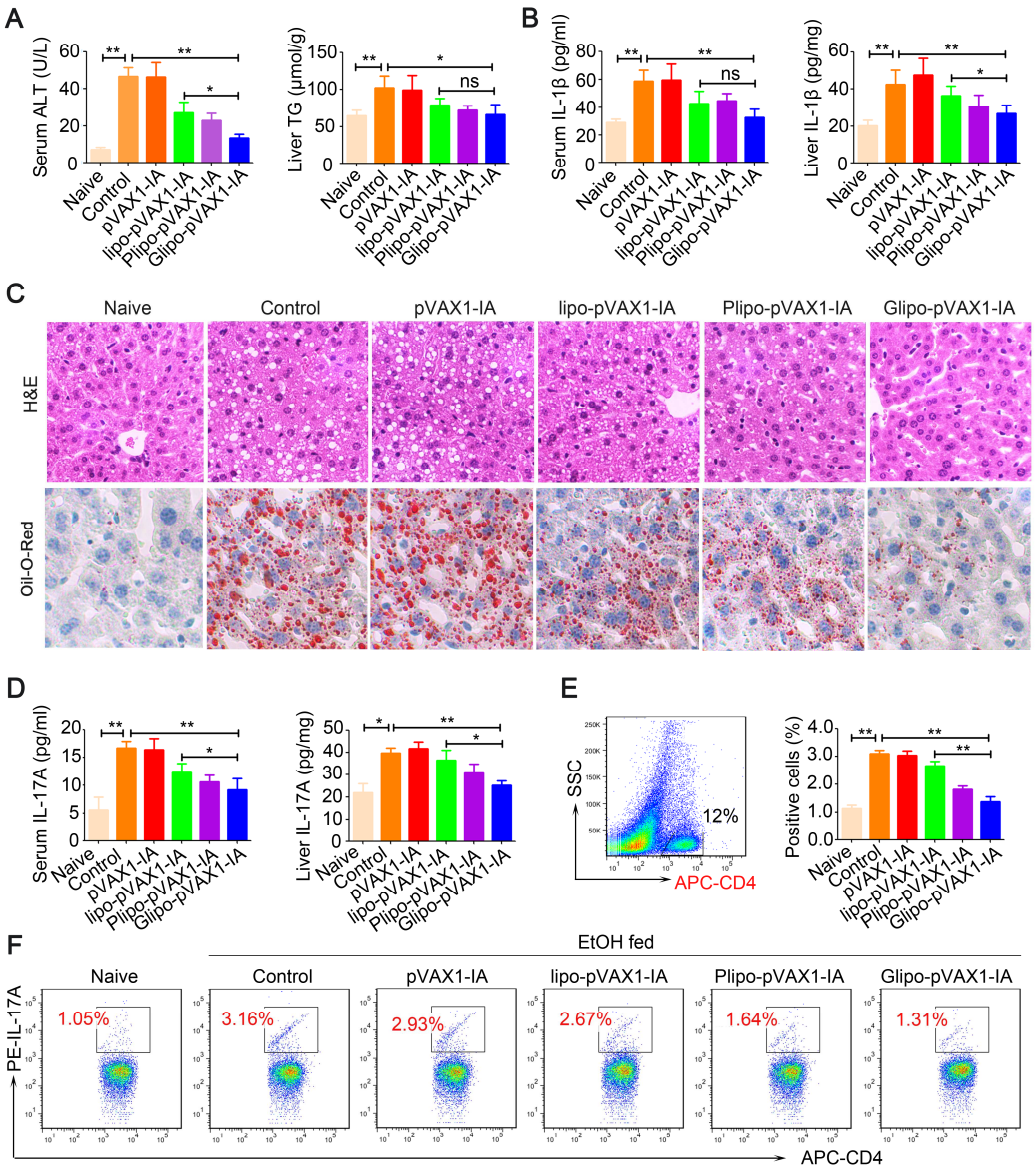

Fig. 6. Glipo-pVAX1-IA nanobiologics protected against hepatic inflammatory cells infiltration and liver damage triggered by alcohol feeding. C57 BL/6 mice were exposed to chronic-binge model, and mice undergoing alcohol feeding were treated with PBS (Control group), free pVAX1-IA, lipo-pVAX1-IA, Plipo-pVAX1-IA and Glipo-pVAX1-IA every three day (n = 6 for each group). (**A**) Serum ALT and liver TG levels were analyzed. (**B**) Serum and liver IL-1β levels were measured. (**C**) Liver damage and steatosis were analyzed by H&E and Oil-O-Red staining

(magnification: 400×). (**D**) Levels of IL-17A in the serum and in the liver. (**E**) The CD4-positive cells in nonparenchymal liver cells were sorted by flow cytometry. Quantification of the amount of CD4 and IL-17A-double positive Th17 cells were displayed. (**F**) The frequency of Th17 cells in nonparenchymal liver cells. Data indicated means ± SD, *$p < 0.05$, **$p < 0.01$.

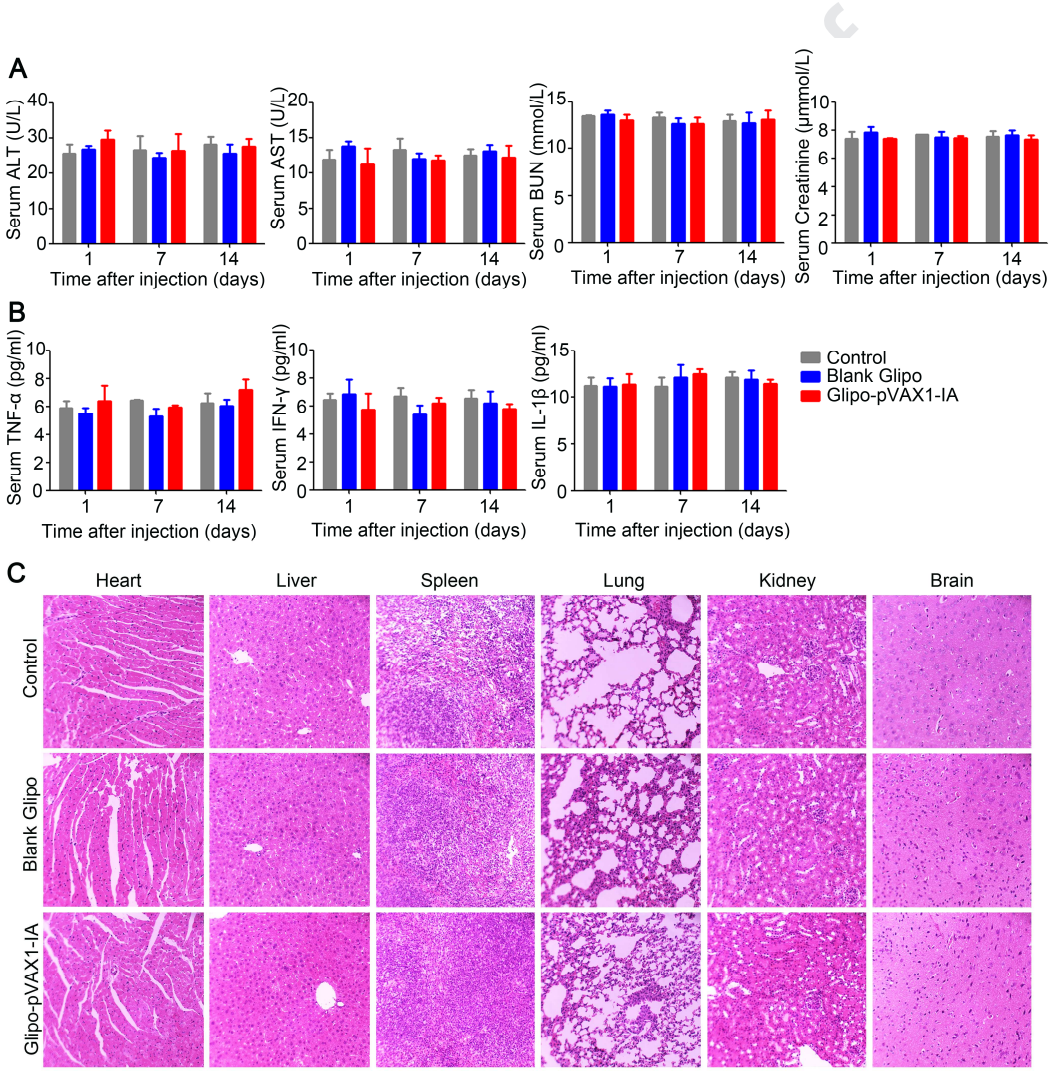

Fig. 7. Administration of Glipo-pVAX1-IA did not cause systemic toxicity in mice. PBS (Control), blank Glipo and Glipo-pVAX1-IA were administrated into mice via vein tail (n = 5 for each group), respectively. Serum samples were collected at 1, 7

and 14 days, and major organs were harvested 14 day post injection. (**A**) Serum ALT, AST, BUN and creatinine were assessed. (**B**) Serum concentrations of TNF-α, IFN-γ and IL-1β. (**C**) Mice were sacrificed on day 14 after injection of nanobiologics and tissue injury was determined by H&E staining (Magnification: × 200). Data indicated means ± SD, *$p < 0.05$, **$p < 0.01$.

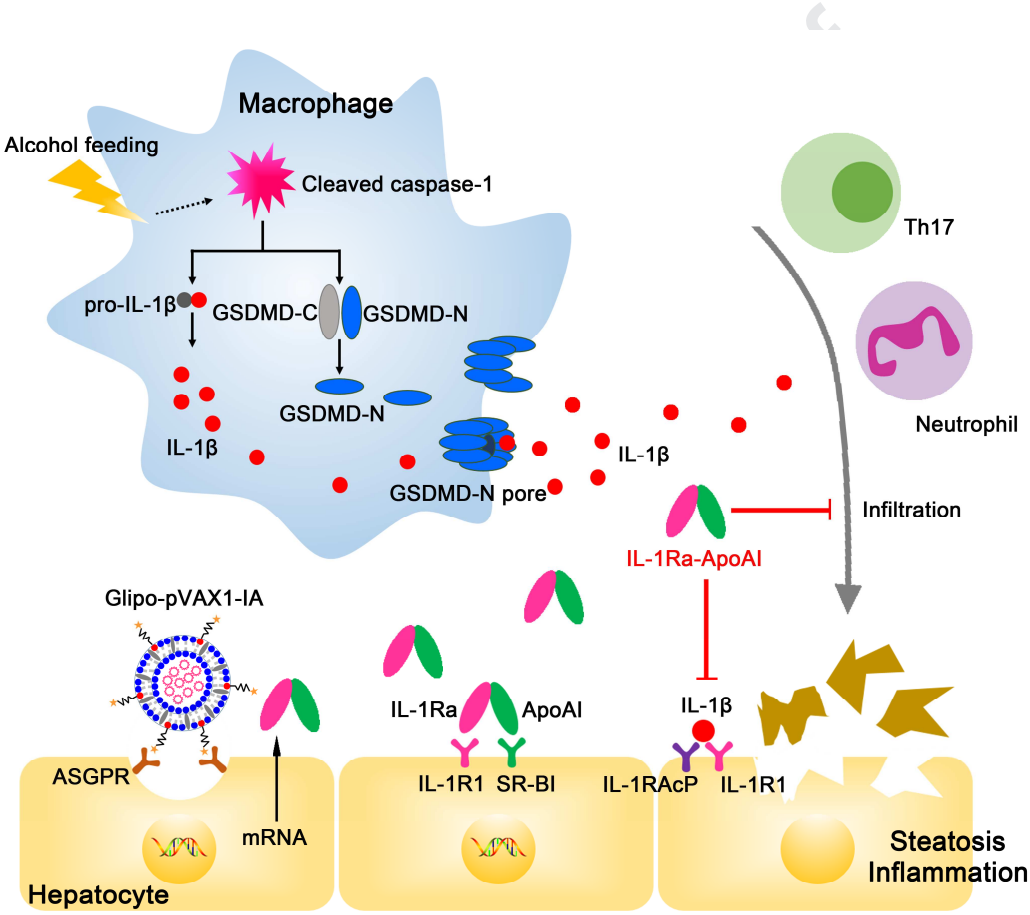

Graphical Abstract Excessive ethanol feeding contributes to the cleavage of caspase-1, which processes the maturation of IL-1β and cleaves inactive GSDMD into active GSDMD-N. GSDMD-N forms pores on the plasma membrane that mediates IL-1β secretion into the cytoplasm. Once released, IL-1β binds to IL-1R1 and IL-1RAcP to induce the hepatocyte damage, as well as infiltrates Th17 cells and

neutrophils into the damaged regions, leading to aggravated liver steatosis and inflammation. Here, we developed the hepatocyte-targeted delivery strategy by packaging pVAX1-IA into galactose-functioned nanobiologics. The resulting Glipo-pVAX1-IA was specifically internalized into hepatocytes by ASGPR-mediated endocytosis and delivered into nucleus for transcription. The fusion protein IL-1Ra-ApoAI was expressed that promotes secondary targeting to hepatocytes by ApoAI-mediated binding with SR-BI receptor, which contributed to the competitive binding of IL-1R1 by IL-1Ra, thus blocking the pathogenic effects of IL-1β and attenuating ASH.

Declaration of interests

☒ The authors declare that they have no known competing financial interests or personal relationships that could have appeared to influence the work reported in this paper.

☐The authors declare the following financial interests/personal relationships which may be considered as potential competing interests: